electronics

MDPI

Article

Distributed Robust Optimization Method for Active Distribution Network with Variable-Speed Pumped Storage

Pengyu Pan [1,2,*], Gang Chen [1,2], Huabo Shi [1,2], Xiaoming Zha [3] and Zhiqiang Huang [3]

[1] State Grid Sichuan Electric Power Research Institute, Chengdu 610041, China; gangchen_thu@163.com (G.C.); shbo87@163.com (H.S.)
[2] Sichuan Key Laboratory of Power Internet of Things, Chengdu 610041, China
[3] School of Electrical Engineering and Automation, Wuhan University, Wuhan 430072, China; xmzha@whu.edu.cn (X.Z.); huangzq@whu.edu.cn (Z.H.)
* Correspondence: ppyswjtu@163.com

Abstract: Variable-speed pumped storage has the advantages of flexible adjustment and low economic cost, which can reduce the adverse effects caused by a high proportion of new energy access. In order to reduce the system operation risk caused by the randomness of new energy output, a distribution robust optimization method for an active distribution network with variable-speed pumped storage is proposed. Firstly, considering the probability distribution uncertainty of wind–solar prediction error, a two-stage distributed robust optimization model of an active distribution network is constructed with the sum of day-ahead operating cost, intra-day adjustment cost expectation and conditional value-at-risk as the objective function. Then, the probability distribution fuzzy set is constructed based on the norm distance, and the fuzzy set boundary is determined by a data-driven method. Finally, the model is transformed into a mixed integer second-order cone optimization model by a linearization method and duality theory, and verified by an example. The results show that the proposed model can effectively reduce the operation risk caused by the uncertainty of operating cost and wind–solar output and reduce the operational costs and the risks associated with uncertainty in wind and solar power output.

Keywords: variable-speed pumped storage; active distribution network; operation risk; distributed robust optimization; mixed integer second-order cone optimization

check for updates

Citation: Pan, P.; Chen, G.; Shi, H.; Zha, X.; Huang, Z. Distributed Robust Optimization Method for Active Distribution Network with Variable-Speed Pumped Storage. *Electronics* **2024**, *13*, 3317. https://doi.org/10.3390/electronics13163317

Academic Editors: Ke Wang, Junyu Chen, Yinbo Ge, Zhuang Xiao and Xiangke Li

Received: 17 July 2024
Revised: 16 August 2024
Accepted: 16 August 2024
Published: 21 August 2024

Copyright: © 2024 by the authors. Licensee MDPI, Basel, Switzerland. This article is an open access article distributed under the terms and conditions of the Creative Commons Attribution (CC BY) license (https://creativecommons.org/licenses/by/4.0/).

1. Introduction

A high proportion of new energy connected to the active power grid will cause problems such as wind–solar abandonment and voltage overstep, and flexible resources are needed to reduce the adverse effects of the uncertainty of new energy output [1]. The combination of electrical automation and new energy technologies improves the operating efficiency while ensuring system stability [2,3]. In recent years, the application of variable-speed pumped storage (VPS) in high-proportion new energy systems has attracted widespread attention [4,5]. VPS stores energy by pumping water from the lower reservoir to the upper reservoir during the load low period, and releases the stored water through turbines to generate electricity during the peak period. VPS can effectively smooth out the volatility of new energy output [6]. China has developed a medium- and long-term plan for pumped storage, with an estimated installed capacity of 62 GW by 2025 and 120 GW by 2023 [7]. Therefore, it is of great significance to study the operation optimization of VPS in an active distribution network.

In order not to be disturbed by the uncertainty of wind–solar power, Conditional Value-at-Risk (CVaR) is widely used in power system uncertainty optimization. In order to improve the absorption rate of new energy and the flexibility of system operation, a comprehensive energy system planning model based on CVaR was established in the literature [8]. In [9], stochastic programming and CVaR were combined and a stochastic

optimization model of multi-type equipment in distribution network considering risk management and control were proposed. Considering the lack of real-time communication in the distribution network, [10] uses the CVaR method to determine the solar reactive power output based on a data-driven approach. The CVaR method requires an assumption about the probability distribution of wind power output, which can be subjective and limit its effectiveness [11].

To overcome the disadvantage of presuming probability distributions, distributionally robust optimization (DRO) has been proposed and widely applied [12]. DRO combines the characteristics of robust optimization and random optimization [13,14], constructs a fuzzy set of probability distribution through historical observation data of scenery, and solves the optimization model when uncertainty variables obey the worst probability distribution in the fuzzy set [15]. In [16], a distribution robust optimization method based on Wasserstein distance was proposed based on a data-driven approach. In [17], considering the interaction scenario between the microgrid and distribution network, a single-stage distribution robust optimization model of microgrid was established. In [18], scene clustering was carried out based on the error data of wind–solar historical prediction, and a two-stage distribution robust optimization model was established based on norm distance considering the uncertainty of the probability distribution of cluster scenes.

DRO considers the average operating cost in the worst case of the probability distribution of wind–solar prediction errors, ignoring the operating risk caused by wind–solar uncertainty, resulting in the risk of high operating costs in some extreme operating scenarios [19]. Most of the existing literature only focuses on DRO or CVaR as a way to deal with wind–solar uncertainty, resulting in overly optimistic decision-making [20]. The two-stage distributed robust optimization model with Conditional Value-at-Risk (TSDRO-CVaR) adds CVaR as an additional metric in a risk-averse way, which can overcome the shortcomings of CVaR being too subjective and avoid excessive operating costs in case of abnormal conditions.

In summary, considering the uncertainty of wind–solar output, a TSDRO-CVaR model of an active distribution network with variable-speed pumped storage is proposed, as shown in Figure 1. Day-ahead operation is optimized as the first stage, intra-day real-time optimization as the second stage, and the sum of the operating cost of the first stage, the adjustment cost of the second stage and their CVaR are taken as the objective function. The optimization model is transformed into a mixed integer second-order cone optimization model by a linearization method and duality theory. At the same time, TSDRO-CVaR provides risk preference factors for decision makers, and the larger the risk preference factor, the higher the risk. Decision makers can flexibly set risk preference factors according to the risk preference to take into account the economy and robustness of the model. Finally, the effectiveness of the proposed model is verified by a numerical example.

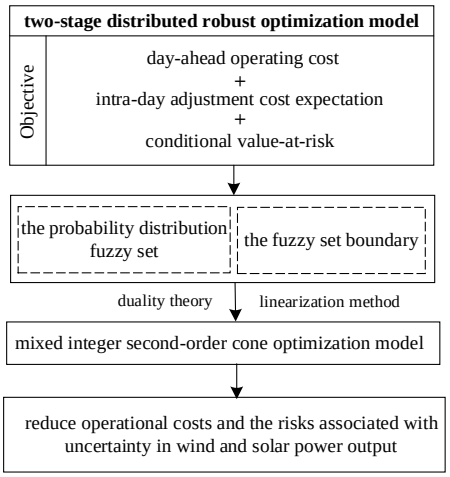


Figure 1. TSDRO-CVaR model of active distribution.

2. TSDRO-CVaR Optimization Model

2.1. TSDRO Model

The objective function of the two-stage robust optimization model is the minimum sum of the expected operating cost of the first stage and the adjustment cost of the second stage. The TSDRO expression is as follows:

$$\min_x F_{ahead}(x) + \sup_{p\in\mathcal{P}} E_p(G(x,\xi)) \tag{1}$$

$$A(x) \le 0 \tag{2}$$

where: x represents the decision variable of the first stage; F_{ahead} represents the day-ahead optimization objective function; ξ represents the uncertain variable, namely the prediction error of the wind–solar power output; p represents the probability distribution function obeyed by the uncertain variable; $\mathcal{P}$ represents the fuzzy set; $E_p(\cdot)$ represents the expectation of obtaining; $G(x,\xi)$ represents the objective function of the second stage, namely the adjustment cost caused by the uncertainty of the wind–solar power output, and the expression is as follows:

$$G(x,\xi) = \min_y F_{Intraday}(y) \tag{3}$$

$$B(x,y,\xi) \le 0 \tag{4}$$

In the formula, y represents the decision variable of the second stage, and $F_{Intraday}(y)$ represents the objective function of intra-day optimization. Formula (4) represents the operational constraint of the model in the second stage.

2.2. TSDRO-CVaR Model

Based on the TSDRO model, the risk cost based on the CVaR method is also considered in the objective function. The objective function of TSDRO-CVaR is as follows:

$$\min_x c^T x + \sup_{p\in\mathcal{P}} \left\{ (1-\lambda) E_p(G(x,\xi)) + \lambda C_{\text{risk}} \right\} \tag{5}$$

where: C_{risk} represents the risk cost caused by the wind–solar power prediction error, and $\lambda \in [0,1]$ reflects that the greater the risk preference factor, the higher the risk. When $\lambda = 0$, the TSDRO-CVaR model was the conventional TSDRO model, and when $\lambda = 1$, Formula (5) was equivalent to the minimum sum of the first-stage operating cost and the wind–solar power uncertain risk cost under the worst distribution.

CVaR comes from the risk value theory and represents the uncertain risk cost caused by the fluctuation of uncertainty variables at a certain confidence level [21]. Based on the CVaR method, when the confidence level is β_C, the calculation formula of uncertain risk cost is as follows:

$$C_{\text{risk}} = \min_\alpha \left\{ \alpha + \frac{1}{1-\beta_C} E_p\left[(G(x,\xi) - \alpha)^+ \right] \right\} \tag{6}$$

$$(G(x,\xi) - \alpha)^+ = \max\{G(x,\xi) - \alpha, 0\} \tag{7}$$

where: α represents the adjustment cost caused by the uncertainty of the wind–solar output prediction when the confidence level is β_C. Finally, the objective function of the TSDRO-CVaR model is as follows:

$$\min_x F_{ahead}(x) + \sup_{p\in\mathcal{P}} \min_\alpha \left\{ \lambda\alpha + E_p[D(x,\xi)] \right\} \tag{8}$$

$$D(x,\xi) = (1-\lambda) G(x,\xi) + \frac{\lambda}{1-\beta_C} (G(x,\xi) - \alpha)^+ \tag{9}$$

3. Two-Stage Robust Optimization Model for Active Distribution Network

3.1. First-Stage Objective Function

$$\min_{x\in X} F_{ahead}(x) = \sum_{t=1}^{T} \left(F_t^{buy} + F_t^{keep} + F_t^{op}\right) \tag{10}$$

where: T represents the total number of day-ahead scheduling periods, take $T = 24$; F_t^{buy} represents the cost of purchasing power from the system to the higher power grid; F_t^{keep} represents the maintenance cost of equipment, including the maintenance cost of wind–solar storage equipment; F_t^{op} represents the operating cost of generator condition change for VPS. The cost of each component is calculated as follows:

$$\begin{cases} F_t^{buy} = c_t P_{t,sub} \\ F_t^{keep} = \sum\limits_{i\in\Omega_{\mathrm{VPS}}} c^{\mathrm{VPS}} \left|P_{t,i}^{\mathrm{VPS}}\right| + \sum\limits_{i\in\Omega_{\mathrm{WT}}} c^{\mathrm{WT}} P_{t,i,pre}^{\mathrm{WT}} \\ \qquad + \sum\limits_{i\in\Omega_{\mathrm{PV}}} c^{\mathrm{PV}} P_{t,i,pre}^{\mathrm{PV}} \\ F_t^{op} = \sum\limits_{i\in\Omega_{\mathrm{VPS}}} c^{op}\left(\left|\mu_{t+1,i,g}^{\mathrm{VPS}} - \mu_{t,i,p}^{\mathrm{VPS}}\right| + \left|\mu_{t+1,i,p}^{\mathrm{VPS}} - \mu_{t,i,p}^{\mathrm{VPS}}\right|\right) \end{cases} \tag{11}$$

where: c_t represents the electricity price at time t; $P_{t,sub}$ represents the power purchased from the distribution network to the superior network at time t; c^{WT}, c^{PV} and c^{VPS} respectively represent the maintenance cost of wind–solar storage per unit output; Ω_{WT}, Ω_{PV} and Ω_{VPS} respectively represent the wind–solar storage installation node collection; Ω_b represents a collection of lines; c^{op} represents the once start-stop operating cost of VPS; $\mu_{t,i,g}^{\mathrm{VPS}}$ and $\mu_{t,i,p}^{\mathrm{VPS}}$ are 0–1 variables, which means that the hydraulic turbine is in the generator state/motor state in the VPS.

3.2. First-Stage Operation Constraint Conditions

(1) VPS Operation Constraints

In the scheduling process, VPS should meet the active power constraint, reactive power capacity constraint, storage boundary constraint and storage daily-constant constraint, that is:

$$\begin{cases} 0 \le P_{t,i,g}^{\mathrm{VPS}} \le u_{t,i,g}^{\mathrm{VPS}} P_{t,i,\max}^{\mathrm{VPS}} \\ -u_{t,i,p}^{\mathrm{VPS}} P_{t,i,\max}^{\mathrm{VPS}} \le P_{t,i,p}^{\mathrm{VPS}} \le 0 \\ u_{t,i,p}^{\mathrm{VPS}} + u_{t,i,g}^{\mathrm{VPS}} \le 1 \\ \sqrt{\left(P_{t,i,g}^{\mathrm{VPS}} - P_{t,i,p}^{\mathrm{VPS}}\right)^2 + \left(Q_{t,i}^{\mathrm{VPS}}\right)^2} \le S_i^{\mathrm{VPS}} \\ V_{t+1,i}^{\mathrm{VPS}} = V_{t,i}^{\mathrm{VPS}} - P_{t,i,g}^{\mathrm{VPS}} \cdot \eta_g^{\mathrm{VPS}} - P_{t,i,p}^{\mathrm{VPS}} / \eta_p^{\mathrm{VPS}} \\ V_{t=T}^{\mathrm{VPS}} = V_{t=0}^{\mathrm{VPS}} \\ V_{i,min}^{\mathrm{VPS}} \le V_{t,i}^{\mathrm{VPS}} \le V_{i,\max}^{\mathrm{VPS}} \end{cases} \tag{12}$$

In Formula (12): $P_{t,i,g}^{\mathrm{VPS}}$ and $P_{t,i,p}^{\mathrm{VPS}}$ respectively represent the active power output of VPS under power generation and pumping conditions; $Q_{t,i}^{\mathrm{VPS}}$ and S_i^{VPS} respectively represent the reactive power output of VPS and the converter limit; η_g^{VPS} and η_p^{VPS} respectively represent the VPS power generation efficiency and pumping efficiency; $V_{t,i}^{\mathrm{VPS}}$ represents the VPS storage capacity at time t; and $V_{i,\min}^{\mathrm{VPS}}$ and $V_{i,\max}^{\mathrm{VPS}}$ represent the minimum and maximum VPS storage capacity.

(2) Power flow constraint

$$\sum_{ij\in\Omega_b} \left(P_{t,ij} - r_{ij} i_{t,ij}\right) + P_{t,i} = \sum_{jk\in\Omega_b} P_{t,jk} \tag{13}$$

$$\sum_{ij\in\Omega_b}\left(Q_{t,ij}-x_{ij}i_{t,ij}\right)+Q_{t,i}=\sum_{jk\in\Omega_b}Q_{t,jk} \tag{14}$$

$$P_{t,i}=P_{t,i,pre}^{\mathrm{WT}}+P_{t,i,pre}^{\mathrm{WT}}+P_{t,i}^{\mathrm{VPS}}-P_{t,i}^{\mathrm{load}} \tag{15}$$

$$Q_{t,i}=Q_{t,i}^{\mathrm{VPS}}-Q_{t,i}^{\mathrm{load}} \tag{16}$$

$$u_{t,i}-u_{t,j}+\left(r_{ij}^2+x_{ij}^2\right)i_{t,ij}-2\left(r_{ij}P_{t,ij}+x_{ij}Q_{t,ij}\right)=0 \tag{17}$$

$$u_{t,i}i_{t,ij}=P_{t,ij}^2+Q_{t,ij}^2 \tag{18}$$

where: $P_{t,ij}$ and $Q_{t,ij}$ respectively represent the active power and reactive power flowing through line ij at time t; $P_{t,i}$ and $Q_{t,i}$ respectively represent the active power and reactive power flowing into node i at time t; r_{ij} and x_{ij} represent the resistance and reactance of line ij; $P_{t,i}^{\mathrm{load}}$ and $Q_{t,i}^{\mathrm{load}}$ respectively represent the active power and reactive power of the load of node i at time t; $u_{t,i}$ and $u_{t,j}$ respectively represent the square of the voltage of nodes i and j at time t; $i_{t,ij}$ represents the square of the current of line ij at time t. Formula (18) is a quadratic equation constraint, which can be converted to the following second-order cone operation constraint by reduction:

$$\left\|\begin{matrix}2P_{t,ij}\\2Q_{t,ij}\\i_{t,ij}-u_{t,i}\end{matrix}\right\|_2\le i_{t,ij}+u_{t,i} \tag{19}$$

(3) Safe operation constraint

$$U_{i,\min}^2\le u_{t,i}\le U_{i,\max}^2 \tag{20}$$

$$0\le i_{t,ij}\le I_{ij,\max}^2 \tag{21}$$

where: $U_{i,\min}^2$ and $U_{i,\max}^2$ respectively represent the square of the minimum and maximum voltage of node i; $I_{ij,\max}^2$ represents the square of the maximum current flowing through line ij.

3.3. Second-Stage Objective Function of Adjustment Operation

In order to reduce the impact of the wind–solar prediction error on the operation economy of the distribution network, the distribution network will implement intra-day control on the dispatchable equipment in the distribution network according to the actual wind–solar output, resulting in intra-day adjustment costs. Due to the existence of wind–solar prediction error, the voltage will exceed the upper/lower limit, and the adjustment of the output of the schedulable equipment may not make the system run in a safe operation state, so it is necessary to abandon wind, solar and load to a certain extent. The objective function of daily adjustment operation is as follows:

$$\min_y F_{Intraday}(y)=\sum_{t=1}^{T}\left(F_t^{u,buy}+F_t^{u,keep}+F_t^{abandon}\right) \tag{22}$$

where: $F_t^{u,buy}$ and $F_t^{u,keep}$ respectively represent the adjustment cost of power purchase and dispatchable equipment of the distribution network from the superior network, and

$F_t^{abandon}$ represents the cost of abandoning wind, solar and load. The specific calculation formula is as follows:

$$\begin{cases} F_t^{u,buy} = c_t\left(P_{t,sub}^{u} - P_{t,sub}\right) + c_{t,d}\left|P_{t,sub}^{u} - P_{t,sub}\right| \\ F_t^{u,keep} = \sum\limits_{i\in\Omega_{\mathrm{VPS}}} c^{\mathrm{VPS}}\left(\left|P_{t,i}^{u,\mathrm{VPS}}\right| - \left|P_{t,i}^{\mathrm{VPS}}\right|\right) + \\ \qquad \sum\limits_{i\in\Omega_{\mathrm{WT}}} c^{\mathrm{WT}}\left(P_{t,i}^{\mathrm{WT}} - P_{t,i,pre}^{\mathrm{WT}}\right) + \\ \qquad \sum\limits_{i\in\Omega_{\mathrm{PV}}} c^{\mathrm{PV}}\left(P_{t,i}^{\mathrm{PV}} - P_{t,i,pre}^{\mathrm{PV}}\right) \\ F_t^{abandon} = c_{t,aban}^{\mathrm{WT}}\left(P_{t,i,real}^{\mathrm{WT}} - P_{t,i}^{\mathrm{WT}}\right) + \\ \qquad c_{t,aban}^{\mathrm{WT}}\left(P_{t,i,real}^{\mathrm{PV}} - P_{t,i}^{\mathrm{PV}}\right) \end{cases} \tag{23}$$

In the formula, $P_{t,sub}^{u}$ represents the actual electricity purchased in the intra-day stage; $c_{t,d}$ represents the penalty coefficient of power change per unit load of the feeder; $P_{t,i}^{u,\mathrm{VPS}}$ represents the output active power of intra-day VPS; $P_{t,i}^{\mathrm{WT}}$ and $P_{t,i}^{\mathrm{PV}}$ respectively represent the dispatching wind–solar power; $P_{t,i,real}^{\mathrm{WT}}$ and $P_{t,i,real}^{\mathrm{PV}}$ respectively represent the actual wind–solar output; $c_{t,aban}^{\mathrm{WT}}$ and $c_{t,aban}^{\mathrm{WT}}$ respectively represent the penalty cost of abandoning wind–solar at time t.

3.4. Second-Stage Operation Constraint Conditions

During intra-day actual operation, the real-time power of WT and PV will deviate from the day-ahead predicted power, and the output of the schedulable equipment must be changed in real time on the basis of the day-ahead variable to meet the power-flow balance. However, the 0-1 state variables of the system operation are not included, including the operating condition of the VPS and the operating state of the contact switch. This is because once VPS operating states are determined in the day-ahead phase, they are difficult to change in the real-time phase.

In order to reduce the influence of the wind–solar output prediction error, the operation optimality can be re-realized by dispatching the output of the dispatchable equipment in the distribution network. Through the linear affine tunable strategy [22], real-time variables in the distribution network can be associated with relevant day-ahead variables, and a constraint model related to real-time variables can be constructed. Equipment output adjustment constraints mainly include VPS output adjustment constraints, namely:

$$\begin{cases} P_{t,i,g}^{u,\mathrm{VPS}} = P_{t,i,g}^{\mathrm{VPS}} + a_{t,i,g}^{P}\xi_t \\ P_{t,i,p}^{u,\mathrm{VPS}} = P_{t,i,p}^{\mathrm{VPS}} + a_{t,i,p}^{P}\xi_t \\ Q_{t,i,pp}^{u,\mathrm{VPS}} = Q_{t,i,g}^{\mathrm{VPS}} + a_{t,i,g}^{Q}\xi_t \\ Q_{t,i,pp}^{u,\mathrm{VPS}} = Q_{t,i,p}^{\mathrm{VPS}} + a_{t,i,p}^{Q}\xi_t \\ Q_{t,i,pp}^{u,\mathrm{VPS}} = Q_{t,i,gp}^{\mathrm{VPS}} + a_{t,i,gp}^{Q}\xi_t \\ Q_{t,i,pp}^{u,\mathrm{VPS}} = Q_{t,i,pp}^{\mathrm{VPS}} + a_{t,i,pp}^{Q}\xi_t \end{cases} \tag{24}$$

where: ξ_t represents the sum of the wind–solar prediction errors of the system at time t; a is the affine tunable coefficient.

The intra-day stage decision variable is affine coefficient a. In order to avoid scheduling difficulties caused by the excessive power adjustment of the equipment, the affine coefficient meets the following constraints:

$$-1 \le a_t \le 1 \tag{25}$$

The constraints of the intra-day stage are similar to those of the day-ahead stage, except that 0–1 state variables in the day-ahead stage do not change in the intra-day stage, and all day-ahead continuous variables in the day-ahead stage are replaced by real-time continuous variables, and specific constraints are not repeated [23].

The TSDRO-CVaR model established in this paper belongs to the min-max-min three-layer two-stage optimization problem, the upper layer is the day-ahead optimization problem, the mid-layer is the probability distribution function for the intra-day forecast error scenario optimization problem, and the lower layer is the intra-day optimization problem. A schematic diagram of a three-layer two-stage optimization model is shown in Figure 2.

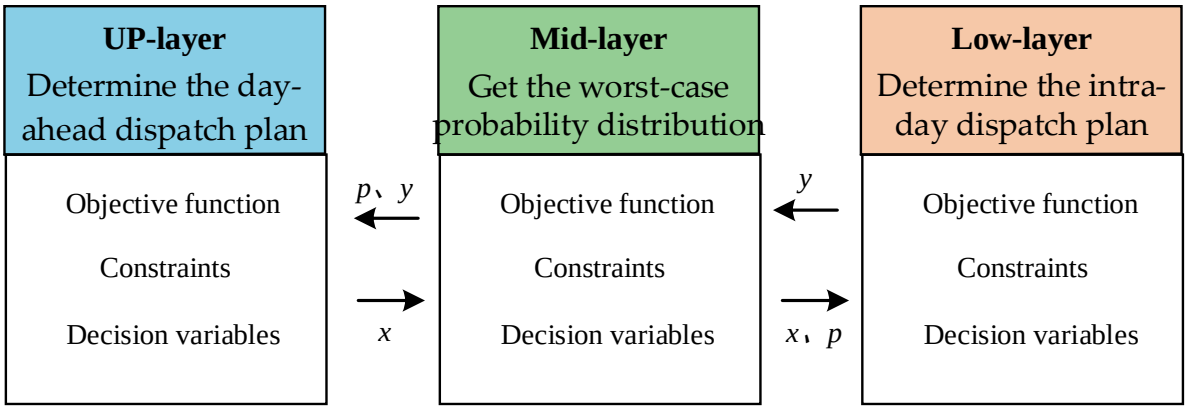


Figure 2. Schematic diagram of a three-layer two-stage optimization model.

4. Solution of TSDRO-CVaR Model

4.1. Construction of Probability Distribution Fuzzy Set Based on Data Driven Method

Based on the data-driven method, the historical errors of N scene-power prediction were clustered, using K-means clustering with the number of clusters as the parameter. To obtain m actual scenarios, the reference probability distribution of different scenarios was p^0. Due to the uncertainty of prediction, there is error between the reference probability distribution p^0 and the actual probability distribution p, and the fuzzy set P is defined using the confidence set of 1-norm and ∞-norm, which is defined as follows:

$$\mathcal{P} = \left\{ p \geq 0, \left\| p - p^0 \right\|_1 \leq d_1, \left\| p - p^0 \right\|_\infty \leq d_\infty, 1^T p = 1 \right\} \tag{26}$$

where: distribution $\|\cdot\|_1$ and $\|\cdot\|_\infty$ respectively represent the 1-norm and ∞-norm; d_1 and d_∞ respectively represent the 1-norm deviation and ∞-norm deviation allowed by the probability distribution; 1 represents the column vector with each element being 1. Then the objective function (8) can be expressed as:

$$\min_x F_{ahead}(x) + \sup_{p \in \mathcal{P}} \min_{\alpha} \left\{ \lambda \alpha + \sum_{i=1}^{m} p_i D(x, \xi^i) \right\} \tag{27}$$

The confidence of the probability distribution p can be expressed as:

$$\Pr\left\{ \left\| p - p^0 \right\|_1 \leq d_1 \right\} \geq 1 - 2me^{-2Nd_1/m} \tag{28}$$

$$\Pr\left\{ \left\| p - p^0 \right\|_\infty \leq d_\infty \right\} \geq 1 - 2me^{-2Nd_\infty} \tag{29}$$

Let the confidence degrees to the right of Formulas (28) and (29) be β_1 and β_∞, then d_1 and d_∞, whose true distribution and reference distribution can be calculated as follows:

$$d_1 = \frac{m}{2N} \ln \frac{2m}{1 - \beta_1} \tag{30}$$

$$d_\infty = \frac{1}{2N} \ln \frac{2m}{1 - \beta_\infty} \tag{31}$$

4.2. Model Transformation

The TSDRO-CVaR model belongs to a three-layer non-convex optimization model, and the main solution methods include the C&CG algorithm and Bender decomposition method. However, the iterative solution of the main problem and sub-problem has the problems of long solution time and slow convergence speed. The proposed model is converted to a mixed integer linear programming model for solving by duality theory and linearization, which can accelerate the model solving speed. Since the TSDRO-CVaR model about variables p and variables α are convex optimization problems, according to the strong duality theory, max and min are exchanged to obtain the objective function of TSDRO-CVaR:

$$\min_{x,\alpha} F_{ahead}(x) + \lambda\alpha + \max_{p\in\mathcal{P}} \sum_{i=1}^{m} p_i D(x,\xi^i) \tag{32}$$

The auxiliary variable h is introduced to linearize the fuzzy set $\mathcal{P}$, and the corresponding dual variable is introduced. The specific expression is as follows:

$$\mathcal{P} = \begin{cases} p - p^0 \le h \perp \theta \ge 0 \\ p^0 - p \le h \perp \gamma \ge 0 \\ h \le d_\infty 1 \perp \omega \ge 0 \\ 1^T h \le d_1 \perp z \ge 0 \\ 1^T p = 1 \perp \pi \\ p, h \ge 0 \end{cases} \tag{33}$$

where: θ, γ, ω, z and π are the dual variables corresponding to each constraint in the fuzzy set. Based on the Lagrange duality principle, the dual problem of the variable p in the TSDRO-CVaR optimization model is as follows:

$$\min F_{ahead}(x) + \lambda\alpha + d_1 z + d_\infty 1^T\omega + \pi + (\theta - \gamma)^T p^0 \tag{34}$$

$$s.t. \begin{cases} A(x) \le 0 \\ \theta_i - \gamma_i + \pi \ge D(x,\xi^i) \\ z + \omega_i - \theta_i - \gamma_i \ge 0 \\ \theta, \gamma, \omega, z \ge 0 \end{cases} \tag{35}$$

Since $D(x,\xi^i)$ contains a nonlinear term, auxiliary variables v_i are introduced to linearize it:

$$v_i \ge G(x,\xi^i) - \alpha \tag{36}$$

$$v_i \ge 0 \tag{37}$$

Then Formula (35) can be described as:

$$s.t. \begin{cases} A(x) \le 0 \\ z + \omega_i - \theta_i - \gamma_i \ge 0 \\ v_i \ge G(x,\xi^i) - \alpha \\ \theta_i - \gamma_i + \pi \ge (1-\lambda) G(x,\xi^i) + \frac{\lambda}{1-\beta_C} v_i \\ z, \omega, \theta, \gamma, v \ge 0 \end{cases} \tag{38}$$

After using duality theory and a linearization method, TSDRO-CVaR appears as a single layer optimization model, but because of the existence of constraints $G(x,\xi^i)$, TSDRO-CVaR is still a double layer model. Since the objective function in Formula (34) is linearly positively correlated with variables θ, γ and π, the fourth inequality constraint in Formula (38) will obtain an equal sign when the optimal solution is obtained. Considering

that the objective function $G(x,\xi^i) \geq F_{Intraday}(y^i)$ of the intra-day stage optimization model is always true, Formula (38) can be rewritten as follows by shrinking:

$$s.t.\begin{cases} A(x) \leq 0 \\ B(x,y^i,\xi^i) \leq 0 \\ z+\omega_i-\theta_i-\gamma_i \geq 0 \\ v_i \geq F_{Intraday}(y^i)-\alpha \\ \theta_i-\gamma_i+\pi \geq (1-\lambda)F_{Intraday}(y^i)+\frac{\lambda}{1-\beta_C}v_i \\ z,\omega,\theta,\gamma,v \geq 0 \end{cases} \tag{39}$$

Since $F_{ahead}(x)$ and $F_{Intraday}(y^i)$ are linear objective functions about variables, and $A(x) \leq 0$ $g(x,y^i,\xi^i) \leq 0$ are second-order cone optimization constraints, the final TSDRO-CVaR model is converted to a mixed-integer second-order cone optimization model.

5. Examples and Result Analysis

The model established in this paper belongs to the mixed integer linear programming model, which uses Matlab 2020b and invokes Mosek's second-order cone optimization solver under the compilation support of YALMIP. The optimized computer hardware parameters are as follows: the processor is an 11th Gen Intel(R) Core(TM) i7-11800H; the main CPU frequency is 2.30 GHz; the disk is a 512 solid state drive; the running speed of RAM is 3200 MHz; the size is 16 GB; the operating system is Windows10 64 bit.

5.1. Scenarios and Parameters

In order to verify the advantages of the proposed model in reducing system operating costs and uncertain risks, the improved IEEE69 node system, as shown in Figure 3, was selected for analysis. The voltage operating safety range was 0.95 p.u.~1.05 p.u; the rated load of the system was 9505 kW + j6767 kVar; the line impedance of the system is 2/5 that of a standard 69-node system. The installed nodes and installed capacity of distributed power supply in the distribution network are shown in Table 1. The total distributed power generation is 3400 kW, accounting for 35.8% of the total load of the system. The prediction results of wind power, photovoltaic, load and time-divided price are shown in the literature [24].

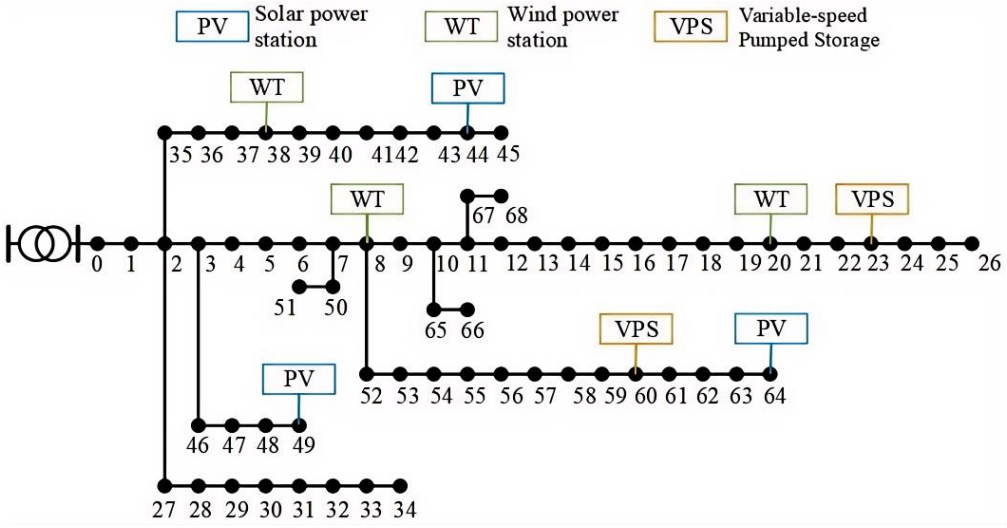


Figure 3. Improved IEEE69 node system.

Table 1. Paragrams of DGs.

Species	Wind Power			Solar Power		
Position	8	20	38	44	49	64
Capacity [kW]	400	400	400	1000	600	600

The installed nodes of VPS units are 23 and 60; the parameters of the two VPS units are the same; the rated power is 2 MW; the reservoir capacity is 4.8 × 104 m^3; the minimum storage capacity is 10% of the capacity; the rated water head is 100 m; and the VPS operating efficiency is 90%.

It is assumed that the prediction error probability distribution function of the wind and photovoltaic in the system meets the positive distribution, and the prediction error does not exceed 20% of the prediction output. Stratified sampling was carried out for the wind–solar prediction error: the number of selected error samples was 1000; the number of clusters was 10; the confidence level of fuzzy set construction and CVaR were 90%; the risk appetite coefficient was 0.5.

5.2. Correlation Analysis of Different Optimization Models

(1) Compared with robust optimization RO and random optimization SO

In order to verify the superiority of the TSDRO-CVaR model, the SO and RO models of the distribution network are established respectively for solving. TSDRO-CVaR and SO are calculated based on 10 samples obtained by clustering, and RO carried out interval optimization with 20% of the wind–solar prediction output as the fluctuation range. The solution results of the three models under different sample sizes are shown in Figure 4. The RO model ignores the historical data of the wind–solar prediction error and considers making decisions in the worst case, but the distribution of the prediction error in actual operation is far less than the worst-case distribution, so the RO model will cause the highest operating cost of the distribution network. The SO model finds the operation strategy with the minimum expected cost under various scenarios, but due to the limited number of samples, the theoretical probability distribution of SO has a certain deviation from the actual probability distribution, thus resulting in the lowest operating cost of the distribution network. The operating cost of TSDRO-CVaR is between RO and SO, and as the number of samples increases, the results of the model become smaller and smaller.

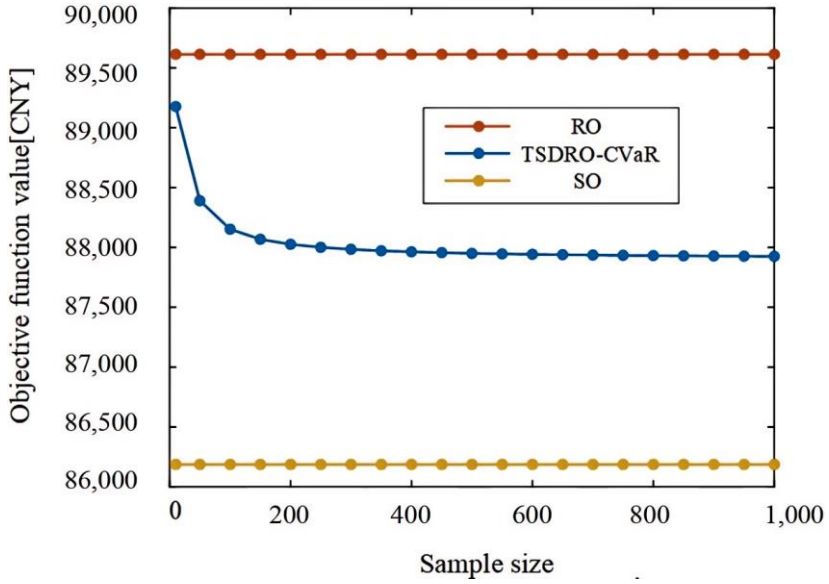


Figure 4. Operating costs of RO, TSDRO-CvaR and SO models.

(2) Compared with TSDRO and CVaR optimization models

In order to compare the results of the TSDRO-CVaR model with those of the TSDRO and CVaR models, the following randomized experiment was set up: First, 10,000 experimental error samples were randomly selected from existing samples by a stratified sampling method, and the actual total operating cost of the two models was calculated respectively. The difference between the actual operating cost and the operating cost obtained by model optimization was obtained by subtraction, which was called economic risk. The smaller the economic risk, the stronger the capability of wind–solar output uncertainty. The simulation experiment results are shown in Figure 5. In the figure, the economic risk value of TSDRO-CVaR is lower than that of CVaR and TSDRO, indicating that TSDRO-CVaR has a better ability to deal with the uncertainty of the wind–solar. Because the CVaR method only considers the risk of deterministic probability distribution, without considering the uncertain risk of probability distribution, and the TSDRO model only considers the uncertainty of data probability after clustering, without considering the risk cost caused by the uncertainty of wind–solar power. Then, the TSDRO-CVaR model considers the risk cost of uncertain probability, sacrificing some of the economic benefits to obtain better robustness, with stronger anti-interference ability, thus resisting the operating conditions of worse wind–solar uncertainty.

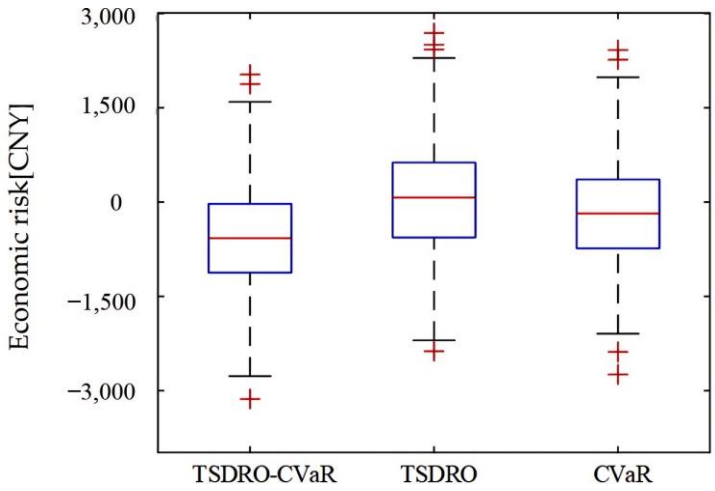


Figure 5. Economic risks of RO, TSDRO-CvaR and SO models.

5.3. Parameter Analysis of TSDRO-CVaR Model

5.3.1. Analysis of Risk Avoidance Factors

When the confidence level is 0.9, the operating cost of the distribution network under different risk appetite factors is shown in Table 2. With an increase in the risk preference factor, the day-ahead dispatching cost and total dispatching cost of the distribution network will increase, and the economy of the system will become worse. The reason is that the greater the risk appetite factor, the more conservatively the decision makers tend to make decisions; in the day-ahead optimization, enough spare capacity will be prepared to deal with the uncertainty of the wind–solar prediction, and at this time the equipment operating costs will be reduced resulting in a decline in day-ahead operating costs. In addition, with the increase in risk appetite factor, the expectation of intra-day adjustment cost will gradually increase, the risk value will gradually decrease, and the robustness of the system will be better. This is because the greater the risk appetite factor, the greater the weight of the risk value in the objective function, and the greater the uncertainty considered in the system decision-making, which means that the adjustment cost expectation and the risk value both become larger.

Table 2. Operating costs of different risk appetite factors.

λ	Day-Ahead Operating Cost [CNY]	Expectations of Intra-Day Adjustment Cost [CNY]	Conditional Risk Value [CNY]	Total Cost [CNY]
0.2	84,768	852	5461	86,542
0.4	85,123	923	4772	87,586
0.6	85,611	1212	3612	88,263
0.8	86,202	1653	3008	88,939
0.99	86,785	1923	2795	89,571

5.3.2. Sample Size Influence Analysis

In order to verify the validity of the data-driven fuzzy set construction method, different sample numbers are selected to construct the prediction error sample set. Figure 6 shows the relationship between ∞-norm distance, the objective function value and the number of samples. As the number of samples increases, the ∞-norm distance of the fuzzy set decreases, so does the objective function value. The reason is that when the scope of the fuzzy set is reduced, the estimated distribution of the error is close to the true distribution, the uncertainty to be dealt with is weakened, and the conservatism of the optimization results is reduced, which indicates that the model in this paper is data-driven and robust. The larger the number of samples, the lower the conservatism of the model. In addition, it can be seen that when the data volume is greater than 200, the system operating cost decreases at a lower rate.

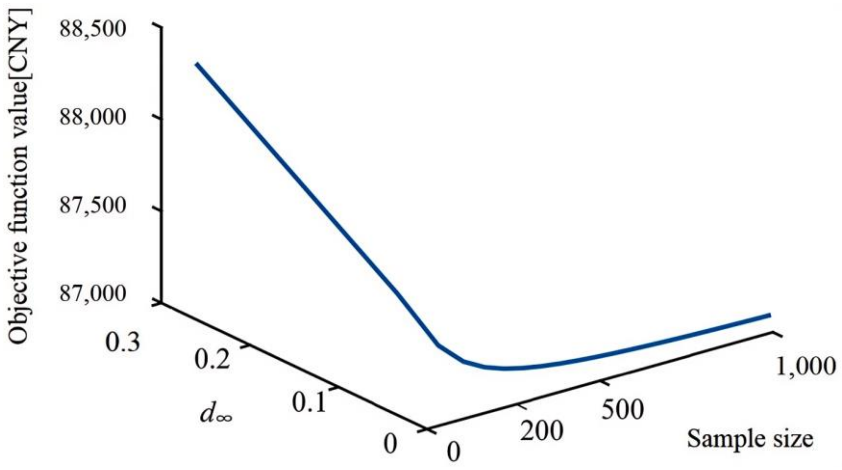


Figure 6. The relationship between norm distance and operating cost under different sample sizes.

5.3.3. Influence Analysis of Different Confidence Levels

According to the objective Function (32), the confidence level of the fuzzy set will affect the size of the fuzzy set, and the confidence level of CVaR will affect the risk cost. Since fuzzy set construction is affected not only by the confidence level but also by the number of samples, in order to highlight the influence of β_1 and β_∞, it is assumed that the number of samples is 200 and $\beta_1 = \beta_\infty$, then the model optimization results under different confidence interval combinations are obtained, as shown in Figure 7. With an increase in confidence level, the operation scheduling cost increases gradually. In addition, it can be seen that when the number of samples is large, the confidence level of CVaR has a greater impact on the objective function.

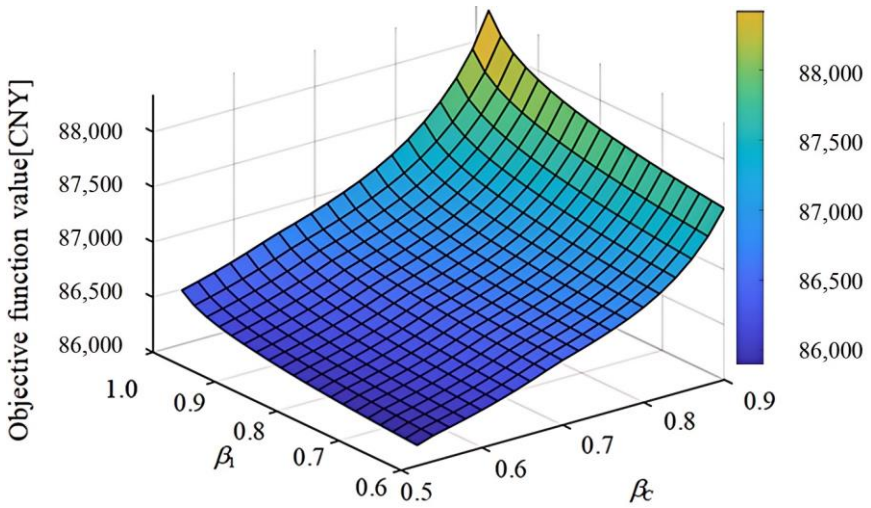


Figure 7. Operating costs under different combinations of confidence levels.

5.4. Comparison of Different Solutions of TSDRO-CVaR Model

In order to verify the speediness and effectiveness of converting the three-layer model into mixed integer linear programming model using the linearization method and duality theory, the solution method in this paper is compared with the Bender decomposition method and the C&CG algorithm. The results are shown in Table 3. It can be seen that the final system operation cost obtained using the three methods is almost the same. However, the calculation time of the proposed method is 37.6% and 32.8% of that of the Bender decomposition method and C&CG algorithm, respectively, indicating the rapidness of the proposed method.

Table 3. Comparison of the results of different solution methods.

	Calculation Time [s]	**Operating Costs [CNY]**
Bender decomposition method	51.6	87,927
C&CG algorithm	45.0	87,927
Method from this paper	16.9	87,926

6. Conclusions

The paper addresses the system operation risks associated with high proportions of renewable energy integration by proposing an active distribution network distributionally robust optimization method based on variable-speed pumped storage. By considering the probabilistic distributional uncertainty of wind and solar forecast errors, a two-stage distributionally robust optimization model is developed and converted into a mixed-integer second-order cone programming model for solution. Finally, the improved IEEE69 node distribution network is used to solve and verify the calculation example. The results are as follows:

(1) The TSDRO-CVaR model introduces CVaR as an additional metric, overcomes the disadvantages of SO being too optimistic and RO being too conservative, and has stronger anti-risk ability compared with TSDRO and CVaR models.
(2) Using a linearization method and duality theory, the model is converted into a mixed integer second-order cone model for solving, and the calculation speed is significantly faster than that of the Bender decomposition method and C&CG algorithm.

The active distribution network distributionally robust optimization method proposed in this paper, with its comprehensive cost and risk optimization strategy, provides an effective solution for distribution network operation in the context of high proportions

of renewable energy integration. Future research could further explore the application potential and scalability of this method in more complex power system environments.

The distribution network considered in this paper contains only one dispatching resource—VPS, and the collaborative optimization of multiple types of dispatchable resources in the distribution network needs further research.

Author Contributions: Literature search, study design, data analysis and manuscript writing, Z.H., P.P. and X.Z.; supervision, project administration and funding acquisition, P.P., H.S. and G.C. All authors have read and agreed to the published version of the manuscript.

Funding: This research was funded by the Science and Technology Project of State Grid Sichuan Electric Power Company under Grant 521997230002.

Data Availability Statement: Data are contained within the article.

Conflicts of Interest: The authors declare no conflicts of interest.

References

1. Zhang, Z.; Zhang, Y.; Huang, Q.; Lee, W.J. Market-oriented Optimal Dispatching Strategy for a Wind Farm with a Multiple Stage Hybrid Energy Storage System. *CSEE J. Power Energy Syst.* **2018**, *4*, 417–424. [CrossRef]
2. Chen, J.; Hu, H.; Wang, M.; Ge, Y.; Wang, K.; Huang, Y.; Yang, K.; He, Z.; Xu, Z.; Li, Y.R. Flow Control-Based Regenerative Braking Energy Utilization in AC Electrified Railways: Review and Future Trends. *IEEE Trans. Intell. Transp. Syst.* **2024**, *25*, 6345–6365. [CrossRef]
3. Chen, J.; Zhao, Y.; Wang, M.; Wang, K.; Huang, Y.; Xu, Z. Power Sharing and Storage-Based Regenerative Braking Energy Utilization for Sectioning Post in Electrified Railways. *IEEE Trans. Transp. Electrif.* **2024**, *10*, 2677–2688. [CrossRef]
4. Ni, J.; Zhang, Y.; Shi, H. Pumped Storage Quantification in Promoting New Energy Consumption Based on Time Series Production Simulation. *Power Grid Technol.* **2023**, *47*, 2799–2809.
5. Jiang, H.; Du, E.; Zhu, G.; Huang, J.; Qian, M.; Zhang, N. Review and Prospect of Seasonal Energy Storage for Power System with High Proportion of Renewable Energy. *Autom. Electr. Power Syst.* **2020**, *44*, 194–207.
6. Sina, M.; Alireza, A. Daily Performance Optimization of a Grid-connected Hybrid System Composed of Photovoltaic and Pumped Hydro Storage (PV/PHS). *Renew. Energy* **2020**, *159*, 272–285.
7. Juntao, Z.; Chuntian, C.; Shen, Y. Research Progress, Challenges and Prospects of Research on Hydropower Supporting the Flexibility of New Power System. In Proceedings of the CSEE, Harbin, China, 22–24 September 2023.
8. Li, Z.; Wang, C.; Li, B.; Wang, J.; Zhao, P.; Zhu, W.; Yang, M.; Ding, Y. Probability-Interval-Based Optimal Planning of Integrated Energy System With Uncertain Wind Power. *IEEE Trans. Ind. Appl.* **2020**, *56*, 4–13. [CrossRef]
9. Xu, C.B.; Yang, X.D.; Zhang, Y.B.; Zhang, K.Y.; Wang, X.Z.; Tang, M. Stochastic Operation Optimization Method for Active Distribution Networks with Soft Open Point Considering Risk Management and Control. *Autom. Electr. Power Syst.* **2021**, *45*, 68–76.
10. Ayyagari, K.S.; Gonzalez, R.; Jin, Y.; Alamaniotis, M.; Ahmed, S.; Gatsis, N. Learning Reactive Power Control Polices in Distribution Networks Using Conditional Value-at-Risk and Artificial Neural Networks. *J. Mod. Power Syst. Clean Energy* **2023**, *11*, 201–211. [CrossRef]
11. Mengxue, W.; Fang, F. Distributionally Robust Optimization of Electricity-Heat-Hydrogen Integrated Energy System with Wind and Solar Uncertainties. *Trans. Electrotech. Soc.* **2023**, *38*, 3473–3485.
12. Bozorgavari, S.A.; Aghaei, J.; Pirouzi, S.; Nikoobakht, A.; Farahmand, H.; Korpås, M. Robust Planning of Distributed Battery Energy Storage Systems in Flexible Smart Distribution Networks: A Comprehensive Study. *Renew. Sustain. Energy Rev.* **2020**, *123*, 109739. [CrossRef]
13. Gang, D.; Dongmei, Z.; Xin, L. Research Review on Optimal Scheduling Considering Wind Power Uncertainty. *Proc. CSEE* **2023**, *43*, 2608–2626.
14. Rayati, M.; Bozorg, M.; Cherkaoui, R.; Carpita, M. Distributionally Robust Chance Constrained Optimization for Providing Flexibility in an Active Distribution Network. *IEEE Trans. Smart Grid* **2022**, *13*, 2920–2934. [CrossRef]
15. Siqin, Z.; Niu, D.; Li, M.; Gao, T.; Lu, Y.; Xu, X. Distributionally Robust Dispatching of Multi-community Integrated Energy System Considering Energy Sharing and Profit Allocation. *Appl. Energy* **2022**, *321*, 19. [CrossRef]
16. Du, N.; Liu, Y.; Liu, Y. A New Data-Driven Distributionally Robust Portfolio Optimization Method Based on Wasserstein Ambiguity Set. *IEEE Access* **2021**, *9*, 3174–3194.
17. Cao, J.; Zeng, J.; Liu, J.; Xue, F. Distributionally Robust Optimization Method for Grid-connected Microgrid Considering Extreme Scenarios. *Autom. Electr. Power Syst.* **2022**, *46*, 50–59.
18. Ding, T.; Yang, Q.; Yang, Y.; Li, C.; Bie, Z.; Blaabjerg, F. A Data-Driven Stochastic Reactive Power Optimization Considering Uncertainties in Active Distribution Networks and Decomposition Method. *IEEE Trans. Smart Grid* **2018**, *9*, 4994–5004. [CrossRef]
19. Ordoudis, C.; Nguyen, V.A.; Kuhn, D.; Pinson, P. Energy and Reserve Dispatch with Distributionally Robust Joint Chance Constraints. *Oper. Res. Lett.* **2021**, *49*, 291–299. [CrossRef]

20. Cao, Y.; Wei, W.; Mei, S.; Shafie-Khah, M.; Catalao, J.P.S. Analyzing and Quantifying the Intrinsic Distributional Robustness of CVaR Reformulation for Chance-Constrained Stochastic Programs. *IEEE Trans. Power Syst.* **2020**, *35*, 4908–4911. [CrossRef]
21. Yang, Y.; Li, Z.; Mandapaka, P.V.; Lo, E.Y. Risk-Averse Restoration of Coupled Power and Water Systems with Small Pumped-hydro Storage and Stochastic Rooftop Renewables. *Appl. Energy* **2023**, *339*, 14. [CrossRef]
22. Zhao, H.; Wang, X.; Li, B.; Si, Q.; Zhao, M. Distributionally Robust Optimal Dispatch for Multi-community Photovoltaic and Energy Storage System Considering Energy Sharing. *Autom. Electr. Power Syst.* **2022**, *46*, 21–31.
23. Wang, Y.; Yang, Y.; Fei, H.; Song, M.; Jia, M. Wasserstein and multivariate linear affine based distributionally robust optimization for CCHP-P2G scheduling considering multiple uncertainties. *Appl. Energy* **2022**, *306*, 118034. [CrossRef]
24. Huang, Z.; Chen, Y.; Mao, Z.; Sun, J.; Zha, X. Joint Access Planning of Soft Open Point and Distributed Energy Storage System. *Autom. Electr. Power Syst.* **2022**, *46*, 29–37.

Disclaimer/Publisher's Note: The statements, opinions and data contained in all publications are solely those of the individual author(s) and contributor(s) and not of MDPI and/or the editor(s). MDPI and/or the editor(s) disclaim responsibility for any injury to people or property resulting from any ideas, methods, instructions or products referred to in the content.